Evolution, 2023, **77(3)**, 893–906
https://doi.org/10.1093/evolut/qpad004
Advance access publication 13 January 2023
Original Article

Decoupling of height growth and drought or pest resistance tradeoffs is revealed through multiple common-garden experiments of lodgepole pine

Yang Liu[1,2,3,4,5,*], Nadir Erbilgin[6], Eduardo Pablo Cappa[7,8], Charles Chen[9], Blaise Ratcliffe[1], Xiaojing Wei[6], Jennifer G. Klutsch[6,10], Aziz Ullah[6], Jaime Sebastian Azcona[6,11], Barb R. Thomas[6], Yousry A. El-Kassaby[1]

[1]Department of Forest and Conservation Sciences, University of British Columbia, Vancouver, British Columbia, Canada
[2]McDonald Institute for Archaeological Research, University of Cambridge, Cambridge, United Kingdom
[3]Wolfson College, University of Cambridge, Cambridge, UK
[4]Queensland Alliance for Agriculture and Food Innovation (QAAFI), Centre for Crop Science, University of Queensland, St. Lucia, Queensland, Australia
[5]ARC Centre of Excellence for Plant Success in Nature and Agriculture, School of Biological Sciences, University of Queensland, St. Lucia, Queensland, Australia
[6]Department of Renewable Resources, University of Alberta, Edmonton, Alberta, Canada
[7]Instituto Nacional de Tecnología Agropecuaria (INTA), Instituto de Recursos Biológicos, Centro de Investigación en Recursos Naturales, Hurlingham, Buenos Aires, Argentina
[8]Consejo Nacional de Investigaciones Científicas y Técnicas (CONICET), Buenos Aires, Argentina
[9]Department of Biochemistry and Molecular Biology, 246 Noble Research Center, Oklahoma State University, Stillwater, OK, United States
[10]Natural Resources Canada, Canadian Forest Service, Northern Forestry Centre, Edmonton, Alberta, Canada
[11]Irrigation and Crop Ecophysisology Group, Instituto de Recursos Naturales y Agrobiología de Sevilla, Sevilla, Spain

*Corresponding author: Queensland Alliance for Agriculture and Food Innovation (QAAFI) and ARC Centre of Excellence for Plant Success in Nature and Agriculture, University of Queensland, St. Lucia, Queensland 4072 Australia. Email: y.liu4@uq.edu.au

Abstract

The environment could alter growth and resistance tradeoffs in plants by affecting the ratio of resource allocation to various competing traits. Yet, *how* and *why* functional tradeoffs change over time and space is poorly understood particularly in long-lived conifer species. By establishing four common-garden test sites for five lodgepole pine populations in western Canada, combined with genomic sequencing, we revealed the decoupling pattern and genetic underpinnings of tradeoffs between height growth, drought resistance based on $\delta^{13}C$ and dendrochronology, and metrics of pest resistance based on pest suitability ratings. Height and $\delta^{13}C$ correlation displayed a gradient change in magnitude and/or direction along warm-to-cold test sites. All cold test sites across populations showed a positive height and $\delta^{13}C$ relationship. However, we did not observe such a clinal correlation pattern between height or $\delta^{13}C$ and pest suitability. Further, we found that the study populations exhibiting functional tradeoffs or synergies to various degrees in test sites were driven by non-adaptive evolutionary processes rather than adaptive evolution or plasticity. Finally, we found positive genetic relationships between height and drought or pest resistance metrics and probed five loci showing potential genetic tradeoffs between northernmost and the other populations. Our findings have implications for deciphering the ecological, evolutionary, and genetic bases of the decoupling of functional tradeoffs due to environmental change.

Keywords: common-garden approach, *Dendroctonus ponderosae*, *Endocronartium harknessii*, tradeoffs, *Pinus contorta*, resource allocation

Introduction

The tenet of the life-history theory is that the total resource allocated to survival, growth, and reproduction is limited, and thus allocation to each life-history trait is constrained by tradeoffs among traits that have arisen as a consequence of natural selection (Agrawal et al., 2010; Schluter et al., 1991; Stearns, 1999). Long-lived woody perennial plants, such as coniferous trees, must acquire and allocate limited resources such as carbohydrates to increase biomass and to withstand various biotic and abiotic stressors, creating potential tradeoffs in resource allocation among different traits (Niinemets, 2010). At the phenotypic level, tradeoffs between growth and resistance can influence competitive ability and stress resistance (Kempel et al., 2011; Lind et al., 2013; Strauss et al., 2002), manifesting their fundamental plant life-history strategies (Grime, 1979; Raffa et al., 2017). On the other hand, adaptation to the local environment involves genetic tradeoffs between fast growth and resistance to stressors, for instance, growth vs. cold hardiness[1] (Aitken & Bemmels, 2016; Leites

1 The ability of tissues to withstand cold temperatures by preventing ice formation inside the cells.

Received July 19, 2021; revisions received December 15, 2022; accepted January 12, 2023

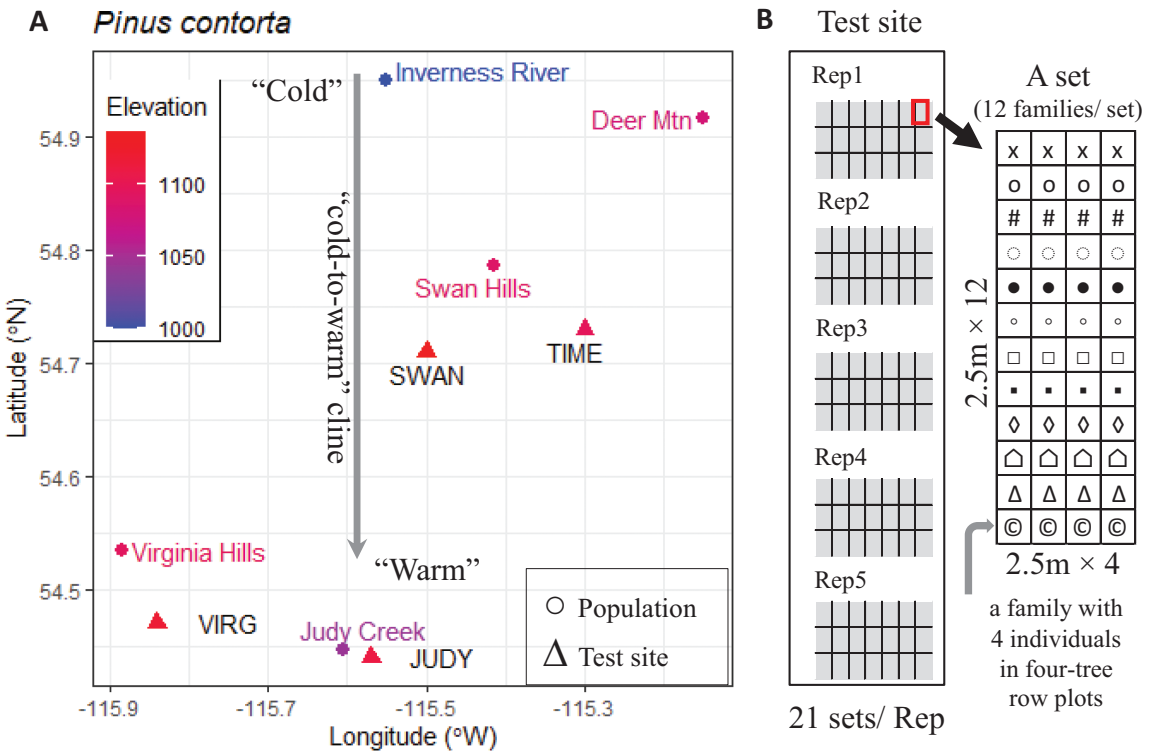

Figure 1. Field sites and experimental design of *Pinus contorta*. (**A**) Geographic coordinates of five study populations (filled circles) and four progeny test sites (triangles). Full location names are used for population sites, and four capital letters represent a test site throughout the study. According to site mean annual temperature (Supplementary Figure S1 and Supplementary Table S1), we defined that "cold-to-warm" test sites are TIME, SWAN, VIRG, and JUDY, respectively; "cold-to-warm" populations are Inverness River, Deer Mtn, Swan Hills, Virginia Hills, and Judy Creek, respectively. A cold-to-warm cline was depicted on the graph. (**B**) Each test site followed sets nested in replicate design, containing a total of five replicates in each site. Each replicate contained 21 sets with 12 families per set and four individuals per family planted in a 2.5 m grid.

et al., 2019), growth vs. pathogen (McKown et al., 2014) or herbivory (Coley et al., 1985; Fine et al., 2004) resistance, and growth vs. survival (Bigler & Veblen, 2009; Wright et al., 2003). However, climate change can affect interactions among these traits by directly affecting photosynthesis (e.g., decreased photosynthesis due to drought) or indirectly regulating pest populations (e.g., accelerated insect development due to warming) (Trumbore et al., 2015). Currently, there is a limited understanding of the extent to which changing environments could alter resource allocation between growth traits and biotic and abiotic resistance under stressful conditions. Likewise, it is less known how evolutionary processes influence, and genetic tradeoffs might constrain, such a change.

Resource allocation theory (Barton & Koricheva, 2010; Boege et al., 2007) suggests that plants optimize defensive resource allocation between growth and defense traits depending on the available resources. Continuous resource allocation is particularly critical for trees that constantly grow. Recent research on growth vs. defense highlights the outcome of functional tradeoffs between primary and secondary metabolisms in conifers (Erbilgin et al., 2021; Huang et al., 2020; Hussain et al., 2020), as resource availability can affect the evolution of the plant metabolites by modulating the cost-benefit ratio of defenses. Typically, resource-abundant environments (e.g., warm, wet, nutrient-rich) select for higher growth rates at the expense of defenses against pests, because tissue damage by herbivores or pathogens becomes less costly to fitness in such environments; in contrast, resource-poor and stressful environments select for slow growth, with high tissue value and thus greater defense (Coley et al., 1985; Endara & Coley, 2011). Consequently, the magnitude of functional tradeoffs alters by leveraging the ratio of resource allocation to growth and defense through molecular regulation.

In this study, we selected five populations of lodgepole pine (*Pinus contorta* Dougl. ex. Loud. var *latifolia* Englm.) established in four common-garden progeny trial test sites (Figure 1A). The populations and test sites were arrayed in a cold-to-warm cline based on temperature (Supplementary Table S1). Our goal was to examine the pattern, evolutionary cause, and genetic basis of changes in trait coordination at test sites to elucidate the hierarchical allocation of resources to several phenotypic traits at the mature tree stage (>35 yr) in multiple different environments, including tree height growth, drought resistance based on water-use efficiency inferred from carbon isotope composition ($\delta^{13}C$) and dendrochronological analysis, and metrics of pest resistance based on host suitability to two most abundant pest species. Western gall rust (WGR; *Endocronartium harknessii* Hirats.) is an important fungal disease on lodgepole pine and widespread across the study region. The second pest studied is the mountain pine beetle (MPB; *Dendroctonus ponderosae* Hopkins)—one of the most important agents of lodgepole pine mortality in western North America (e.g., [Erbilgin, 2019; Raffa et al., 2008]). Specifically, we sought to test for the following three hypotheses: (a) the decoupling of height growth and $\delta^{13}C$ or pest resistance metrics tradeoffs occurs more likely in cold (stressful) relative to warm (favorable) growing conditions; (b) evolutionary processes driving population divergence modulate

functional tradeoffs with population variation; and (c) trait coordination is shaped by a common genetic basis of multi-trait associative variants and genetic tradeoffs.

Considering the resource allocation hypothesis, resource investment in plant resistance would increase in environmentally stressful conditions due to limited resources available. We, therefore, expect that height growth and $\delta^{13}C$ tradeoffs mitigate or even switch to synergistic relationships in cold test sites. On the contrary, more resource allocation to height growth would gain greater fitness benefits under favorable conditions, pushing lower investment in $\delta^{13}C$ and thus maintaining or even steepening their tradeoffs in warm test sites. Due to the specificity, conditionality, and complexity of pest attacks (Erbilgin, 2019), we do not expect a pronounced increase in resource allocation to pest resistance in cold test sites and thus a clinal change in the height and pest resistance relationship along test sites.

In quest of understanding functional tradeoffs to various degrees in the study populations, we assume that a population may be composed of phenotypically plastic genotypes, which produce different phenotypic trait values in fluctuating environments (Gavrilets & Scheiner, 1993; Moran, 1992); alternatively, a population may consist of genetically differentiated individuals, each having fixed phenotypes across environmental conditions (Moran, 1992). Either plastic strategy allows a population to adjust trait coordination with environmental variation. Evidence has revealed that adaptive, plastic, and neutral evolutionary processes drive phenotypic divergence in forest trees (Albert et al., 2011; Kawecki & Ebert, 2004). We, therefore, expect that both phenotypic plasticity and evolutionary mechanisms (divergent/stabilizing selection, gene flow, and/or genetic drift) drive populations with variable responses in trait coordination under changing environments.

Finally, by modeling trait relationships based on genetic variants peak associated with both height and focal resistance traits, we investigated the idea of a common genetic basis of functional coordination. As a locus can have more than two functionally distinct haplotypes (allelic heterogeneity), there are numerous examples of genetic clines along environmental gradients that are related to phenotypic trait variation (e.g., a plant defense locus *GS-ELONG* [Züst et al., 2012] and flowering time variation loci—*FRIGIDA* locus and its epistatic interaction with the *FLC* locus [Caicedo et al., 2004; Stinchcombe et al., 2004]). A dual role of a locus is also reflected by increasing fitness via one trait but reducing it through a second; as such, the locus has pleiotropically antagonistic effects (Rose, 1983) causing functional tradeoffs. Here, we want to identify single nucleotide polymorphisms (SNPs) that are likely subjected to functional tradeoffs between cold vs. warm populations, whereby finding corresponding genes harboring those SNPs.

Material and methods

Plant material and experimental design

We selected five lodgepole pine provenances (populations hereafter), representing a total of 224 maternal half-sib families, grown in four progeny test sites (>35 yr) located along various climatic gradients in central Alberta, Canada (53–59 families from each site used for this study; Supplementary Table S1). All families were divided into 21 sets, each consisting of about 12 families. At each site, the field design was sets nested in five replicates with 21 sets per replicate, and families within each set were planted in four-tree row plots at a 2.5 × 2.5 m spacing (Figure 1B). All sites were fenced and each trial had a border row of trees around the outside. Across the four progeny test sites, we chose a total of 1,490 trees for genotyping and phenotyping.

Variant calling and genotyping

Current year needles from all 1,490 trees were collected in the summer of 2017 (35 yr) and stored at −80 °C until being transported to Alberta Innovates in Vegreville (aka InnoTech Alberta) for DNA extraction. Genomic DNA was extracted using a DNeasy 96 Plant Kit (Qiagen, Germany) and the quality of DNA was assessed to ensure a minimum of 30 µl at 30–100 ng/µl. Genotyping-by-sequencing (GBS) was then conducted on an Illumina HiSeq2000 at the Institute of Biotechnology, Cornell University, following a previous procedure (Chen et al., 2013; Elshire et al., 2011) with restriction enzyme *Pst-1* (CTGCAG). Due to the lack of a lodgepole pine reference genome, SNP determination was performed by aligning the reads with the *Pinus taeda* genome assembly v2.0 with BWA (Li & Durbin, 2009) using TASSEL-GBS (Glaubitz et al., 2014). Aligning sequencing reads to the read tags generated 170,166 SNP markers. For the raw SNP table, the mean read depth for all samples was 55.9 (std = 12.3), and 41.4 (std = 44.2) for the SNPs. There was an average of 62.6% of missing data across all loci. SNP data were further filtered by using <70% missingness and minor allele frequency (MAF) >1%, yielding 25,099 (25.1K) SNPs for downstream analyses. Missing data were imputed using the mean allele.

Phenotypic measurements

Detailed phenotypic trait measurement procedures are described in the Supplementary Methods S1. Concisely, height growth (m) was measured at age 35-yr with a clinometer. Carbon isotope ratio ($\delta^{13}C$, in ‰) analysis was performed at Alberta Innovates in Victoria, using outside slabs cut and ground from the 5 mm increment cores taken from the north side of each tree at approximately breast height (1.3 m) at age 35. Samples were analyzed using an established method on a MAT253 Mass Spectrometer with Conflo IV interface (Thermo Fisher Scientific, Waltham, MA, USA) and a Fisons NA1500 EA (Fisons Instruments, Milano, Italy). We assessed the severity of WGR infection in the test sites by a qualitative scoring system with discrete categories ranging from no gall symptoms to deceased (four tiers) for all trees sampled at age 36-yr. We also investigated these trees' suitability for MPB. Host tree suitability to the beetles was evaluated by quantifying defense chemicals (constitutive monoterpenes) using a Gas Chromatography/Flame Ionization Detector (Agilent Tech., Santa Clara, CA, USA) based on cambial tissues collected by a hole punch when trees were actively growing, coinciding with MPB flight in western Canada. Then, we tested the response of MPB tunneling in media amended with various host chemical profiles (relative concentrations and proportions of individual monoterpenes in the mixture) reported by Ullah et al. (2021). A cutoff of four categories was used to classify trees with different MPB suitability levels (see Supplementary Methods S1-(3) for details). This experiment described above only focused on the role of host constitutive monoterpenes on the tunneling/feeding activities of MPB and did not incorporate the induced monoterpenes in beetle responses. In addition, we performed

dendrochronological analysis to calculate drought resistance indices based on changes in tree-ring width before and after a drought event (Supplementary Methods S1-(4)).

Data analysis

Phenotypic adjustments

To adjust phenotypic traits, by removing design and spatial effects, we analyzed each trait in each test site using a spatial model with a first-order autoregressive residual (co)variance structure (AR1 × AR1). The analysis was achieved by the following pedigree-based mixed model with a spatial autocorrelation to predict each trait:

$$y = X\beta + Z_r u_r + Z_s u_s + Z_a u_a + \varepsilon \quad (1)$$

where y is the vector of individual-tree trait observations, β is the vector of fixed effects for populations; u_r is the vector of random replicate effects distributed as $u_r \sim \mathcal{N}(0, I\sigma_r^2)$, where I is the identity matrix and σ_r^2 is the replicate variance; u_s is the vector of random set effects distributed as $u_s \sim \mathcal{N}(0, I\sigma_s^2)$, where σ_s^2 is the set variance; u_a is the vector of random effects that represents the genetic effects distributed as $u_a \sim \mathcal{N}\left(0, A\sigma_a^2\right)$, where A is the average numerator relationship matrix derived from the pedigree information and σ_a^2 is the additive genetic variance; and ε is the vector of random residuals, partitioned into spatially dependent (ξ) and independent (η) components. The residual (co)variance matrix is expressed as $\sigma_\xi^2 [AR1(\rho_{col}) \otimes AR1(\rho_{row})] + \sigma_\eta^2 I$, where σ_ξ^2 is the spatially dependent variance, σ_η^2 is the spatially independent variance, $AR1(\rho)$ is the first-order autoregressive correlation process, ρ_{col} and ρ_{row} are autocorrelation parameters for tree column and row positions in a test site, respectively, and $\otimes$ denotes the Kronecker product. The X, Z_r, Z_s, and Z_a terms denote the incidence matrices for respective model-effects. As we sampled 1–2 trees from each plot, we did not consider plot effects in the model. A log-transformation was applied to WGR and MPB data before the adjustment. The adjusted phenotypic traits were obtained for each tree at each site by subtracting the estimated replicate, set, and autoregressive residual effects (i.e., ξ term in the model). We used the "remlf90" function in breedR ver. 0.12.5 in R ver. 4.0.0 (R Core Team, 2020) to fit the model with the Expectation-Maximization REML algorithm. The adjusted trait data were used for all subsequent analyses.

Phenotype differentiation, correlation, and coordination

We performed one-way ANOVAs (population) to test for phenotypic differentiation for each focal trait and inter-population difference at each test site and all sites pooled using the Tukey's HSD post-hoc method implemented by the "TukeyHSD" function in the R package stats ver. 3.6.2. We used a correlation-based approach to investigate inter-trait relationship for each combination of population and test site. The correlation between traits, X and Y, was calculated as,

$$r(X, Y) = \frac{cov(X, Y)}{\sqrt{var(X)\, var(Y)}}$$

To explore the pattern of trait coordination, we carried out a PCA based on phenotypic data of all four focal traits and genomic data, and performed a clustering analysis (Ward's method) for individuals based on phenotypic data using FactoMineR ver. 2.2 (Lê et al., 2008).

Estimation of phenotypic plasticity

We employed linear mixed effect models (LMMs) for each focal trait to disentangle the genetic (family; G), planting environment (test site; E), and interactions thereof (G × E) effects by estimating the fixed effect of test site and the random effects of family and family-by-test site interaction using the univariate REML-LMMs in the R package lme4 ver. 1.1.23 (Bates et al., 2015). We constructed the model (Equation 2) by specifying random intercepts for the family and family by test site (i.e., G × E) effects, such that the two random effects allow for an overall shift in level for each family and a separate shift for each combination of family and test site.

$$\text{trait} \sim -1 + \text{test\_site} + (1|\text{family}) + (1|\text{family} : \text{test\_site}) \quad (2)$$

Statistical significance was calculated using likelihood-ratio tests for the random effects and an F-test with Satterthwaite-approximation degrees of freedom for the fixed effect using the R package lmerTest ver. 3.1.2 (Kuznetsova et al., 2017). The proportion of variance explained (PVE) was reported for all random effects. We furthermore estimated PVE by fixed and random effects for each trait using the "rptGaussian" function in the R package rptR ver. 0.9.22 (Stoffel et al., 2017). The way this package estimates PVE for an effect can be considered equivalent to a goodness-of-fit or R^2 (Nakagawa and Schielzeth, 2013). We used the same REML-LMM but without the G × E term to compute the PVE for G and E effects, as the interaction effect has been included as part of the test site effect repeatability according to Schielzeth and Nakagawa (2013). We used 5,000 parametric bootstrapping iterations for the confidence interval (CI) estimation and 5,000 permutations for the significance test.

Population genetic structure

To decipher genetic structure, we calculated the pairwise genomic distances between individuals using a Euclidean distance estimated by the "dist" function in the R package stats ver. 3.6.2. We then visualized the genomic distance among individuals by implementing a principal coordinate analysis (PCoA) using the "dudi.pco" function in the R package ade4 ver. 1.7-15 (Dray & Dufour, 2007).

Heritability and test for evolutionary causes of phenotypic divergence

We employed a multi-trait single-site genomic best linear unbiased prediction approach to estimate genetic components, V_A and V_ε, for genomic-based heritability h^2 estimation (Supplementary Methods S2). We used the approach developed by Ovaskainen et al. (2011) to test for signals of phenotypic selection, which allows for differentiating natural selection and genetic drift as the cause of population divergence. This approach first analyzes genotypic data under a neutral model that assumes that the genes coding for a target trait are as divergent as neutral markers (i.e., $Q_{ST} = F_{ST}$). This model therefore considers the population mean genetic additive values to follow a multivariate normal distribution, with the covariance between pairs of population means in proportion to the pairwise average co-ancestry between populations (i.e., neutrality for a trait):

$$A^P \sim \mathcal{N}(0, 2G^A \otimes \theta^P) \quad (3)$$

where A^P is the vector of population means, G^A is the ancestral variance–covariance matrix of the traits in question, and θ^P is the population-to-population co-ancestry matrix.

Subsequently, the approach uses a Bayesian mixed-effects "animal" model for each trait (phenotypic data) to decompose the additive genetic values into population and individual effects.

Prior to the use of the method to compare the probability distribution of predicted and observed mean additive genetic values, we used genotypic data and the admixture *F*-model (AFM) for neutral divergence among populations implemented in the R package RAFM ver. 1.2 (Karhunen & Ovaskainen, 2012) to estimate θ^P and F_{ST} for each pair of populations. The AFM assumes that the current populations are derived from a single non-sampled ancestral population (Karhunen & Ovaskainen, 2012; Ovaskainen et al., 2011). We fitted both AFM and DRIFTSEL models with 85,000 Markov chain Monte Carlo (MCMC) iterations, discarded a burn-in of 55,000 iterations, and thinned the remaining by 30 to provide 1,000 samples from the posterior distribution. Increasing to this sample size was based on the assessment of convergence by drawing the Monte Carlo traces of the co-ancestry coefficients. We conducted three independent runs for each trait and combinations thereof. The presence of selection was determined by a neutrality test based on *S* statistics. The *S* estimates provided the posterior probability that the observed population divergence arises under divergent selection ($S \approx 1$), stabilizing selection ($S \approx 0$) or genetic drift (intermediate *S* values ≈ 0.5) (Ovaskainen et al., 2011). Due to the computational demands of analyzing the full dataset, we used a subset of 3,864 biallelic SNPs for this analysis by imposing more stringent filtering parameters of MAF ≥1%, missingness ≤10%, and DP ≥140 on the 25.1K SNPs.

Phenotype–genotype-environment associations

A genetic relationship matrix (i.e., *G*-matrix) consists of the additive genetic variances and covariances of multiple traits, providing a statistical summary of the amount and shape of genetic variation within populations. It is integral to understanding multivariate evolution in quantitative traits (Lande 1979, 1980). We first generated a *G*-matrix based on the 25.1K SNPs using the VanRaden (2008) method:

$$G = \frac{WW^{\mathrm{T}}}{2\sum_1^{m_i} p_i(1 - p_i)} \quad (4)$$

where W is the SNP marker incidence matrix assuming $W \subset \{-1, 0, 1\}$ and $\mathbf{p_i}$ is the allele frequency of the i^{th} marker present in the W matrix.

To probe putative causal genomic markers underlying trait variation, we carried out genome-wide association study (GWAS) tests using an LMM of the EIGENSTRAT algorithm (Price et al., 2006) and a fixed and random model circulating probability unification (FarmCPU; ref. [Liu et al., 2016]). While the LMM tests one marker at a time, FarmCPU performs marker tests using other associative markers as covariate in a fixed effect model (Liu et al., 2016). The *G*-matrix was used as covariates to account for the relatedness between individuals. As the degree to which growth and pest defenses associated loci vary in effect across space and time (e.g., [Atkinson & Urwin, 2012; Colhoun, 1973; Kelly, 1992]) and the statistical power of detecting associative markers varies with the method used (Solovieff et al., 2013), we selected peak-associated markers for each category of the traits (i.e., height, drought resistance, and pest suitability) at $\alpha = 0.05$ from either GWAS method. We finally retained 335 candidate SNPs peak associated with all three trait categories.

To test whether trait-associated SNPs are under selection by the environment, we used a multivariate association approach—redundancy analysis (RDA; [Legendre & Legendre, 1998]). This is an efficient constrained ordination approach to identify genetic variation underlying local adaptation and has recently been shown to outperform mixed model-based methods, as well as Random Forest, a machine-learning-based method, in identifying loci associated with environmental variation (Capblancq et al., 2018; Forester et al., 2018). Here we performed an RDA to detect SNPs under selection by the climate of origin using the R package VEGAN ver. 2.5-6 (Oksanen et al., 2017). We used the same set of filtered SNPs as in GWAS and climatic data were obtained from ClimateNA ver.6.2.0 (Wang et al., 2016). To reduce the number of climatic variables used, we ran a principal component analysis (PCA) for all climatic variables ($N = 219$) and chose the top 20 climatic variables based on the eigenvector of the first principal component (53.4% of total inertia; Supplementary Figure S10B). Each of these climatic variables had an absolute eigenvalue of no less than 0.788 on the first principal component. The significance of the RDA model was assessed using 9,999 permutations.

Investigation of the genetic basis of trait coordination

As complex traits are governed by many small-effect loci, overlapped associative loci due to selection, pleiotropy or genetic linkage could be used as an indication of shared genetic bases. We used the 335 peak-associated SNPs to investigate genetic bases of focal traits coordination. We constructed generalized additive models (GAM; i.e., generalized linear models with the addition of tensor product smoothing functions of covariates) with an identity link function by using the smallest *p*-values (i.e., strength of association signal) for those selected markers in each trait category, where $-\log(p)$ values for height were modeled as a function of those for drought or pest resistance metrics. We cross validated the model by randomly assigning 75% of the data to train the model and using the remaining 25% for model validation for each of 5,000 bootstrapped model runs. We assessed model fit and reliability by cross-validation statistics (e.g., AIC, explained deviance) and the Pearson's correlation coefficients for each of the bootstrapped samples. The model was implemented using the R package mgcv ver. 1.8.28 (Wood, 2011) and MASS ver. 7.3.51.5 (Venables & Ripley, 2002). In addition, we visualized association signal relationships between traits by performing thin-plate spline nonparametric regressions using the "Tps" function in the R package fields ver.10.3 (Nychka et al., 2015). Smoothing parameters for each spline were chosen to minimize the generalized cross-validation score.

Results

Trait coordination differed in warm vs. cold populations

All traits showed significant differences between populations ($p < .05$) based on one-way ANOVAs (Supplementary Table S2). Tukey's HSD test showed that populations originating from warm sites were different from those from cold sites (e.g., Judy Creek and Virginia Hills vs. Deer Mtn) in height and $\delta^{13}C$ (Supplementary Figure S3). This pattern was corroborated by a PCA, in which the first axis (30% of the inertia) separated Judy Creek and Virginia Hills vs. the other three populations on its positive vs. negative side,

respectively (Supplementary Figure S4A). However, there was no clear interpopulation pattern of the two defense traits. In addition, by clustering all individuals based on focal traits (Supplementary Figure S5A and B), we found that trees taller than 13.9 ± 0.04 m had greater $\delta^{13}C$ (all $p < .05$ in paired comparisons; Supplementary Figure S5C). The infection severity of WGR was less in both tall and short (12.1 ± 0.04 m) trees relative to that of medium-sized (13.1 ± 0.05 m) trees ($p < .05$; Supplementary Figure S5C); small trees appeared to have the highest MPB suitability (Supplementary Figure S5C). Nonetheless, we did not find that individuals from one clustering group pertained to a single population.

Decoupling of functional tradeoffs more likely in cold vs. warm populations and test sites

Pairwise trait correlations showed variation in the size and direction of correlation, depending on population and test site (Figure 2). The three warm populations—Swan Hills, Virginia Hills, and Judy Creek—at test sites geographically proximal to their original locations (Figure 1A) had less changes in correlative magnitude than the two cold populations—Inverness River and Deer Mtn—in the same test sites (Figure 2). The height and $\delta^{13}C$ correlation displayed a gradient in strength and a negative-to-positive change in direction along the warm-to-cold test sites for Inverness River, Virginia Hills, and Judy Creek populations (Figure 2). This clinal pattern was not evident for the correlations between height or $\delta^{13}C$ and either pest (Figure 2). Moreover, the warm test sites (e.g., JUDY and VIRG) were more likely to generate negative correlations between focal traits than cold test sites (e.g., SWAN and TIME) (Figure 2). In addition, host suitability to the two pests had opposite relationships in warm sites across populations except Judy Creek (Figure 2).

Genetic drift drove the phenotypic divergence of study populations

No difference in trait plastic responses among families

We found significant genetic variation among families for all focal traits ($p < .05$; Supplementary Table S3). PVE by family was ca. 30% for height, 15% for $\delta^{13}C$ and WGR, and 10% for MPB (Supplementary Table S3 and Figure 3A), in accordance with high variability in effect size of the family (G) effect (Figure 3B). We note that family was a better choice than population for genetic variation partitioning, as some families from different populations did not show significant trait variation ($p > .05$ using a Scott–Knott test; Supplementary Figure S2). All traits except MPB showed a significant plastic response to test sites ($p < .05$; Supplementary Table S3) and PVE by test sites was relatively high in height (12.5%) and $\delta^{13}C$ (19.3%) (Supplementary Table S3 and Figure 3A). The effect size of test sites for all traits except MPB was significant (Figure 3B). This indicates a plastic response in these traits. However, G × E interactions were not significant in all traits and corresponding PVE was as low as 0%–2.3% (Supplementary Table S3 and Figure 3A and B), indicating that plastic responses did not differ among families.

No remarkedly discrete population structure

The pedigree structure identified through genomic relationships showed that the trees sampled had a mean relatedness coefficient of 0.006 (Supplementary Figure S6). PCoA of the genomic distances between trees showed overlapped variation with little indication of discrete population structure (Supplementary Figure S7). This pattern was similar across all first six PCoA axes (3.6% of the genomic variation explained). Relatively, Judy Creek and Deer Mtn had more differences than the other populations, according to the first four principal components (Supplementary Figure S4B). Furthermore, demographic distances between populations were low ($\theta = 0.134–0.273$; Table 1), indicating globally large effective population size (N_e). The co-ancestry estimates within populations (diagonal elements of the θ^P matrix) indicated that Judy Creek had the lowest θ and thus the highest N_e (Table 1). The highest between-population co-ancestry coefficients were Deer Mtn—Inverness River followed by Deer Mtn—Swan Hills and Inverness River—Judy Creek (Table 1), indicating that the highest gene flow occurred between Deer Mtn and Inverness River and that these two populations had high gene flow with Swan Hills and Judy Creek, respectively. In addition, we estimated a posterior median F_{ST} value of 0.081 with 95% central posterior CI of [0.080, 0.082] across populations (Supplementary Figure S8).

Focal traits under weak natural selection

All traits across test sites had an intermediate heritability of ca. 0.45 on average (Supplementary Table S4), indicating significant additive genetic variation and that these traits are under genetic control. The signal of natural selection by *S* statistics showed that all *S* values of the focal traits and their combinations were ca. 0.5 (Supplementary Table S5), indicating that genetic drift rather than natural selection underpins phenotype-level population differentiation.

Genetic basis of trait coordination

There was an intermediate, positive correlation between height and $\delta^{13}C$ (Pearson's $r = 0.302$, $p < .05$; Figure 4A), whereas correlations between pest suitability and height or pest suitability and $\delta^{13}C$ were relatively low and non-significant (all $|r| < 0.05$, $p > .05$; Figure 4A). Consistently, the number of associative SNPs in height and $\delta^{13}C$ was four to five times as high as that of pest suitability (Figure 4A).

We discovered 335 peak-associated SNPs with all three categories of focal traits (Supplementary Figure S9A). Most of these SNPs had an associative $-\log_{10}(p)$ of 1.7 with each trait category (Supplementary Figure S9B). By fitting association signals using $-\log(p)$ values through a GAM, we found that these SNPs were highly associated with both height and $\delta^{13}C$ (Figure 4B). There were positive correlative trends in pest suitability vs. height or $\delta^{13}C$ ($r = 0.04–0.05$ but $p > .05$), albeit no pronounced pattern or significant relationship (Figure 4B). Cross-validation and a χ^2 goodness-of-fit test confirmed the fit of a normal distribution in our data (Supplementary Table S6), and an intermediate correlation between the predicted and observed associations suggests the ability of the model to capture their primary relationships (Supplementary Table S6). In addition, when contouring $\delta^{13}C$ against suitability to either pest, we found a positive relationship for WGR and negative relationship for MPB (Figure 4C). Further, we probed five variants of different allele frequencies between Deer Mtn and the other four populations, indicating potential genetic tradeoffs between a cold (northernmost) and warm populations (Figure 4D). We found these five loci were located within intergenic region. By searching for the flank genomic sequences (5 Kb) of the five SNPs, we identified a malate dehydrogenase and seven unannotated genes that might have a relatedness with those SNPs.

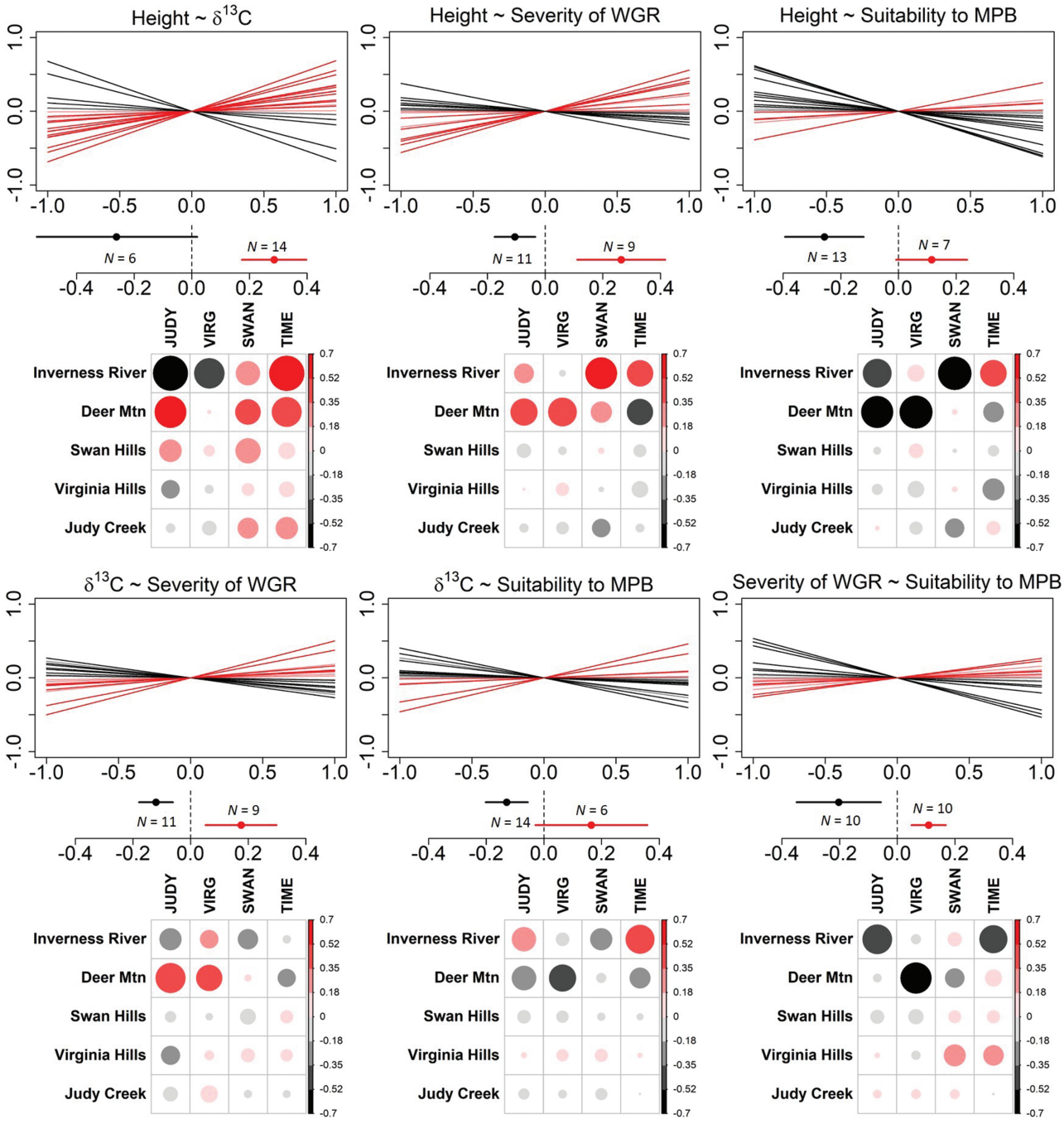

Figure 2. Linear correlation between focal traits of *Pinus contorta* in population by test site. Red and black colors represent positive and negative relationships, respectively. Negative correlations represent phenotypic tradeoffs. Plots in box show the regression lines across all 20 combinations (i.e., five populations × four test sites) using standardized trait values by combination. Beneath are scatter plots with error bars for slope values in positive and negative relationship categories. Heat maps unravel correlations in each population and test site combination in detail. Point size and color depth are proportional to correlative strength.

In addition, we tested whether trait-associated SNPs are under selection by the environment across populations. The RDA model explained a small but significant amount of overall genetic variance (adj. R^2 = 0.07, p < .001 based on a permutation test). The first two axes of the RDA projection represented 23.3% and 21.9% of the explained variance, respectively. Overall, 23.3% of the 25.1K SNPs were outliers and deemed under selection (gray dots in Figure 4E), of which 68 were also associated with focal traits [$-\log_{10}(p)$ > 5.7 and with blue highlight in Figure 4E]. We identified a temperature-based selective gradient corresponding to multiple temperature indexes, such as the top five negatively and positively associated variables with RDA1 (Supplementary Figure S10). Based on allele frequencies of the SNPs under selection, the populations could be classified into two main groups (Supplementary Figure S11), in line with their niche environmental differences (e.g., the two groups of two cold vs. three warm populations).

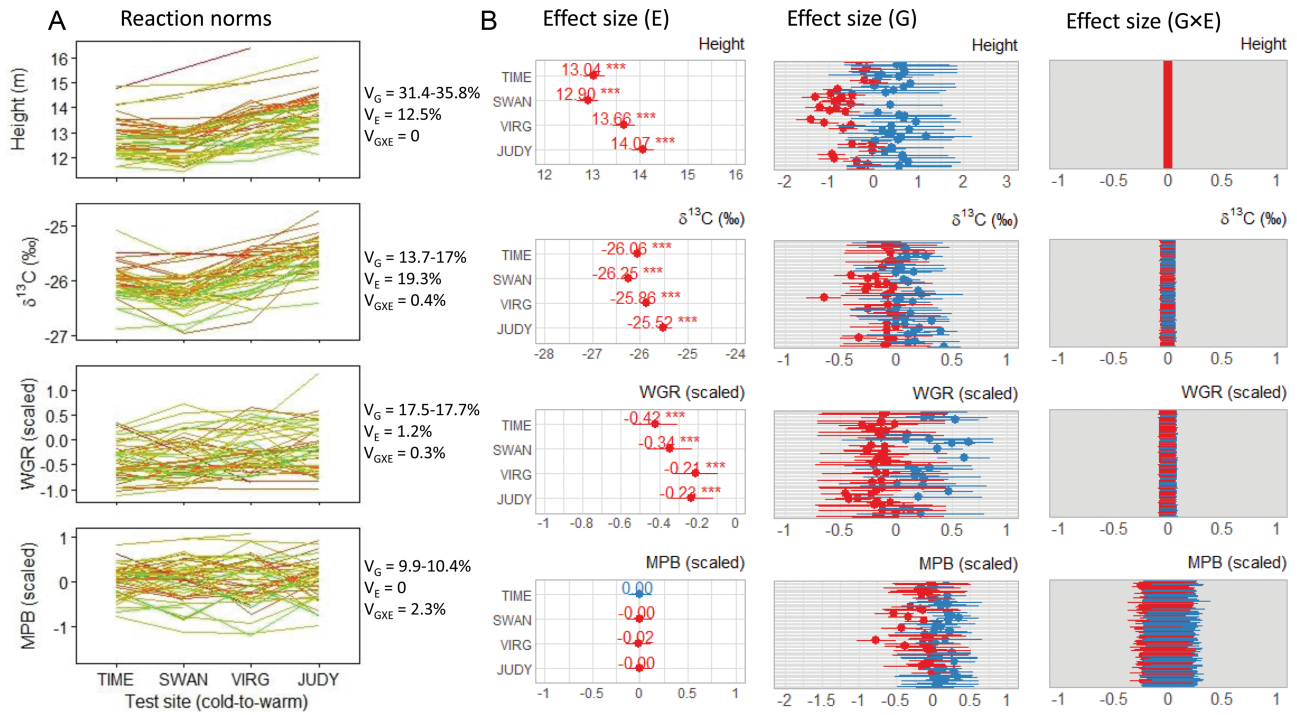

Figure 3. Reaction norms and effect size for family differences in focal traits in the four test sites of *Pinus contorta*. (**A**) Horizontal lines show family-level norms of reaction for a given trait. Families in MAT-decreasing order at site-of-origin are delineated with a red–green gradient on the graph. Percentage of variance explained by family (G), planting environment of test sites (E), and G × E interactions is shown next to each panel. More details about variance decomposition are given in Supplementary Table S6. (**B**) Effect size of G (fixed), E (random), and G × E (random) effects. Red or blue color indicates negative or positive point estimates, respectively. The effect size estimates (G and G × E) are displayed by family horizontally.

Table 1. Co-ancestry matrix of five *Pinus contorta* populations sampled in Alberta, Canada.

Population	Judy Creek	Virginia Hills	Swan Hills	Inverness River	Deer Mtn
Judy Creek	0.134 [0.132, 0.136]				
Virginia Hills	0.080 [0.078, 0.081]	0.138 [0.136, 0.140]			
Swan Hills	0.114 [0.113, 0.115]	0.112 [0.111, 0.113]	0.273 [0.267, 0.280]		
Inverness River	0.125 [0.122, 0.128]	0.122 [0.119, 0.125]	0.107 [0.103, 0.111]	0.233 [0.226, 0.240]	
Deer Mtn	0.097 [0.095, 0.098]	0.095 [0.094, 0.097]	0.125 [0.123, 0.126]	0.141 [0.138, 0.144]	0.141 [0.139, 0.143]

The co-ancestry coefficients (i.e., demographic distance) between populations were estimated by an admixture *F*-model using DRIFTSEL. The diagonal and lower diagonal elements give the within- and among-population co-ancestry coefficients, respectively. Median values are shown with 95% CIs in parentheses.

Discussion

By integrating phenotypic information of trait co-occurrence with genomic analysis, this large-scale study overcame the limitations of space-for-time substitutions (e.g., [Damgaard, 2019; Pickett, 1989]) to elucidate *how* and *why* the decoupling of functional tradeoffs occurs and varies in populations and test sites. While recent efforts have been made to demonstrate variable growth-resistance relationships, we tested for the hypothesis that limited resources in cold test sites are allocated in priority to water-use efficiency ($\delta^{13}C$) at the expense of height growth, leading to flattening tradeoffs or even synergistic relationships. However, resource allocation to pest resistance metrics measured did not vary between cold and warm test sites. We found an opposing trend in two constitutive defenses against WGR and MPB along warm-to-cold test sites. Further, the study populations having functional tradeoffs of different magnitudes are attributable to non-adaptive evolutionary processes (genetic drift and gene flow), rather than phenotypic plasticity or adaptive evolution, which drive the divergence of these populations. Finally, we found positive genetic relationships among height growth, drought, and pest resistance metrics based on the strength of multi-trait peak-association signals. We probed five SNPs of potential genetic tradeoffs between a cold (northernmost) and warm populations and found a dehydrogenase gene that might relate to one such SNP.

Insights into functional coordination: tradeoffs vs. synergies

The current study revealed the decoupling of tradeoffs between height and $\delta^{13}C$ in cold test sites (e.g., SWAN and TIME) across all five lodgepole pine populations investigated and two cold populations (e.g., Deer Mtn and Swan Hills) in warm test sites (e.g., JUDY and VIRG). This indicates that stressful growing conditions (e.g., coldness) could decouple a functional tradeoff and even generate a synergistic relationship, and that variation in population's sensitivity to favorable conditions (e.g., warmness) leads to differences

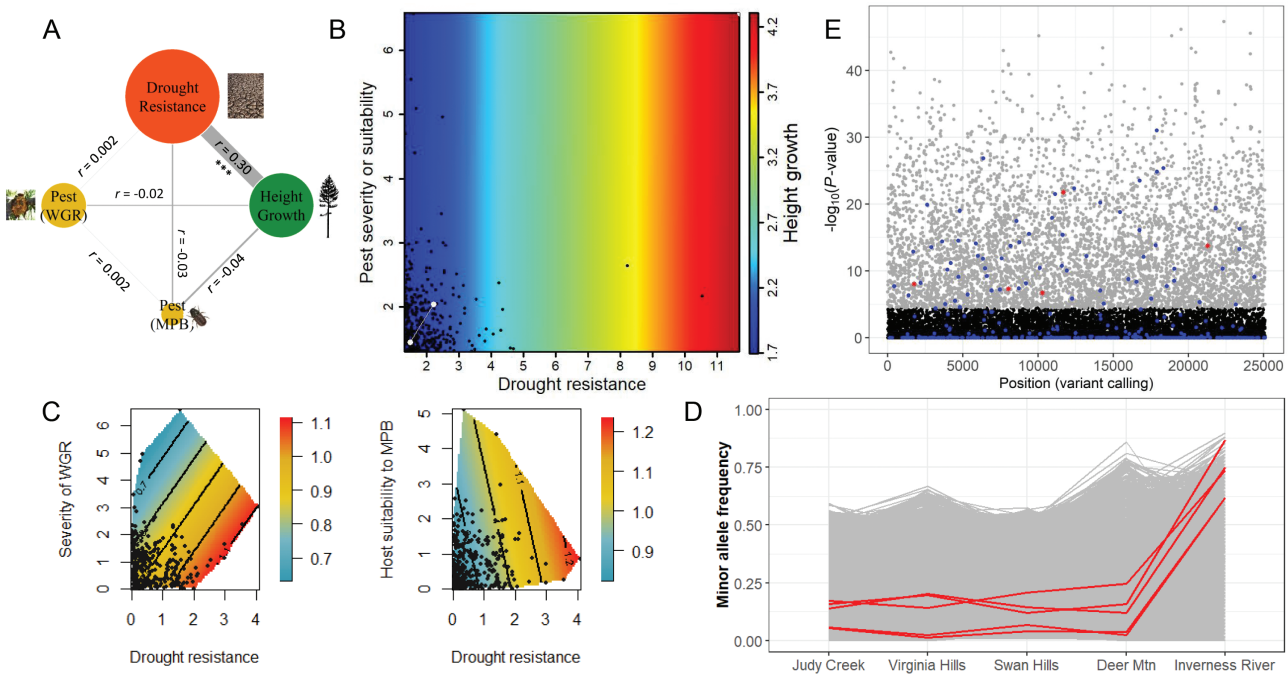

Figure 4. Investigations of the genetic basis of trait coordination and allelic tradeoffs between populations of *Pinus contorta*. (**A**) Pearson's correlation coefficients among four focal traits: height growth, drought resistance, and WGR/MPB pests. The size of nodes indicates the relative genetic basis of each trait (i.e., the number of peak-associated SNPs for each trait in ratio; see Supplementary Figure S9A) and the thickness of edge lines reflects correlation strength. Positive or negative correlations are shown as dark or light gray lines, respectively. (**B**) Contour plot displaying predicted SNP-height association strength by using the strength of associations of the same markers with drought resistance and pest suitability/severity. $-\log_{10}(p)$ values for selected 335 SNPs peak associated with the three categories of traits based on GWAS (Supplementary Figure S9A) were used to construct GAMs (see Supplementary Table S6 for model fit statistics). The 335 data points were marked in black and two white points mark the 25th and 75th percentiles of the data. Density plot for $-\log_{10}(p)$ of these SNPs is displayed in Supplementary Figure S9A. (**C**) Two-dimensional contour plots with colors and contour lines show associations of trait combinations (based on the FarmCPU approach). The color gradient is for height and the 335 data points were marked on the plot. As in (B), axis values and gradient bars are association signals based on $-\log_{10}(p)$; the only difference here is that we considered two pests separately. (**D**) Population mean minor allele frequency by SNP locus. We identified five SNPs with interpopulation $\Delta_{[\text{allelic frequency}]} \geq 0.55$ (i.e., at least more than one allelic difference in a biallelic locus) as highlighted in red. (**E**) Manhattan plot showing the results of SNP-climate associations. Loci under selection by climate, that is $-\log_{10}(p) > 5.7$, are distinguished in gray (N = 5,847), otherwise, in black. The 335 associated SNPs are highlighted in blue, of which 68 SNPs were under selection. The five SNPs showing potential allelic tradeoffs as indicated in (**D**) were marked by red asterisks on the graph. Locus information about the five SNPs includes APFE030845957.1_207031, APFE031507271.1_114818, APFE030130672.1_15992, APFE030586094.1_187779, and APFE030744328.1_248543. Refer to supplemental documents for the upstream/downstream flank genomic sequences (5 Kb) of the five SNPs.

in the magnitude of trait relationships between populations. While a global intraspecies study showed that height and $\delta^{13}C$ were positively correlated (Fardusi et al., 2016), other studies on tree species showed their positive relatedness (e.g. in *Populus* spp. [Gornall & Guy, 2007], *Quercus* spp. [Ramírez-Valiente et al., 2020], and *Betula* spp. [Tenkanen et al., 2019]). Together, prior knowledge agrees with our finding of a positive height-$\delta^{13}C$ correlation in 14 of 20 tests by sites and populations (Figure 2), indicating that increasing $\delta^{13}C$ can compensate for the negative effect of stress due to water deficit. Nonetheless, previous studies have also documented negative genetic correlations between height and $\delta^{13}C$, such as in *P. taeda* (Cumbie et al., 2011) and *Pinus caribaea* (Xu et al., 2000), indicating the underpinning of their potential genetic tradeoffs. Altogether, these results suggest that changes in resource allocation to growth and $\delta^{13}C$ constitutes an important mechanism in mitigating the detrimental effects of stressful growing conditions (e.g., drought or cold spells) on water-use efficiency and tree survival.

Our interpretation about the change to synergistic height-$\delta^{13}C$ relationship in cold test sites was mainly based on the resource allocation hypothesis. From warm-to-cold test sites (JUDY and VIRG vs. TIME and SWAN), height, on average, decreased by 6.6% (Δ = 0.895 m divided by a mean of 13.5 m), whereas the decrement of $\delta^{13}C$ value was only 1.8% (Δ = −0.462‰ over −25.5‰) (calculation based on point effect size estimates in Figure 3B). These results indicate that in cold relative to warm test sites, the extent of decrease in height growth was three times as high as that in water-use efficiency based on $\delta^{13}C$. As such, our finds support that the resources are allocated more to water-use efficiency (i.e., increased ratio of CO_2 assimilation to transpiration) under stressful conditions at the expense of height growth. This change reflects that carbon fixation under stress is used primarily for plant survival rather than vegetative growth.

Whether growth-defense relationships display tradeoffs or synergies depend on the biotic and abiotic context (Züst & Agrawal, 2017). Decoupling of growth-defense tradeoffs could occur by conditionally inducing defense response genes (Karasov et al., 2017). Changes in environmental conditions might give rise to opposite growth-defense relationships over time. Previous findings did not demonstrate tradeoff between

growth and chemical/anatomical defenses in *Pinus* (Kichas et al., 2021; Mason et al., 2019), in part due to strong genetic and environment interactions as suggested by significant correlation for populations in specific test sites but weak correlations across populations and test sites (Figure 2 vs. Figure 4A). Abiotic stress such as drought could limit tree growth, which could reduce resource allocation to defenses (Huang et al., 2020; Hussain et al., 2020; McDowell et al., 2011; Sala et al., 2012). While drought-stressed trees have shown reduced tree defenses against some insect guilds (Bentz et al., 2010; Berner et al., 2017; Kolb et al., 2019), there are other insect guilds that can perform better on well hydrated than drought-stricken trees (e.g. [Kolb et al., 2016]).

Furthermore, there are often instances where resistance to pathogens vs. herbivores diverges (e.g. [Ballhorn, 2011; Erb et al., 2011]). Consistently, our study suggested nearly contrasting patterns in plant responses to pathogenesis vs. herbivory stressors (WGR vs. MPB) along a cold-to-warm test site gradient, indicating that resource allocation to pest resistance varies depending on the resource availability and pest types. These results are expected, as individual pests and their activities are closely tied with specific climatic conditions, such as precipitation and temperature, both of which can differentially influence both host plant susceptibility to organisms and the biology of an organism (Hicke et al., 2012; Jamieson et al., 2012). For example, lodgepole pine stands at high elevations appear to be less suitable to MPB due in part to harmful effects of climate on the beetle biology at higher elevations (Amman & Baker, 1973) and improved defense capacity (Mullin et al., 2021). This agrees with the general idea that plants at lower elevations likely experience higher levels of herbivory and thus select for greater defenses (Galmán et al., 2018; Zangerl & Rutledge, 1996). We observed the highest WGR severity in a wet, warm test site (i.e., VIRG), suggesting that the infection severity is contingent on weather conditions. Broadly, pest species need to survive cold temperatures (i.e., overwintering) such that growth, development, and reproduction can resume when environmental conditions become more favorable. As a result, many pest species have seasonal migration in annual cycles (Chapman et al., 2015) and cold temperatures may become a limiting factor for pest survival and subsequent spread. Furthermore, as infection can expand among trees and might differ between years with different environments, the observed WGR severity is likely a consequence of repeated infection on trees over multiple years.

Other than the environment, genetic differences in pest resistance may result in different host susceptibility to pest species. Indeed, plant responses to a phytopathogen and an insect herbivore (e.g., WGR and MPB) are mediated by different phytohormonal signaling pathways (Erb et al., 2012). The rusts are considered a (hemi-)biotrophic pathogen and plant defenses against biotic pathogens are usually mediated through the salicylic acid-dependent pathway. This pathway leads to the production of antimicrobial molecules (e.g., pathogenesis-related proteins and phytoalexins) and the induction of hypersensitive responses, often associated with programmed cell death in the infected area, which hinders pathogen colonization (Bonello et al., 2006). In contrast, insect herbivory (e.g., MPB) usually triggers jasmonic acid and/or ethylene pathways in plants, resulting in the synthesis of different classes of defense metabolites including terpenes which are important components of tree resistance to bark beetles attacks (Raffa et al., 2008; Ullah et al., 2021). Overall, tree defense against bark beetles is multipartite involving multiple classes of chemical compounds, anatomical, and hypersensitive mechanisms that can be expressed as constitutively or induced (Erbilgin, 2019; Franceschi et al., 2005; Kolosova & Bohlmann, 2012; Raffa et al., 2005). As such, multiple traits operate in unison against various processes and elements of attack instead of a single class of compounds conferring tree resistance against bark beetles.

Lastly, tree size may affect pest-host interacting behavior with smaller trees likely having a lower resistance to pest attacks, but larger trees being more desirable targets on account of their thicker phloem (representing greater resource for colonizing beetles) providing greater nourishment (e.g., MPB cases; ref. [Raffa et al., 2008]). Bark beetles are typically associated with trees with compromised defenses, in line with the trend of the highest MPB suitability in small trees or larger trees attacked by other insects and pathogens. The aforementioned pattern may be applicable only to endemic periods between outbreaks; during outbreaks, MPB does not discriminate between trees with compromised defenses (e.g., [Boone et al., 2011]). In addition, the finding of the highest WGR severity in medium-sized trees suggests a tradeoff between host vulnerability and nutrient availability.

Non-adaptive process modulates population functional tradeoffs of variable magnitudes

Typically, sources of genetic differentiation include adaptive (e.g., natural selection) and non-adaptive (e.g., genetic drift, gene flow, and mutation) evolutionary processes. We identified nearly a quarter of the 25.1K SNPs (23.3%) as imprints of local adaptation, but further results showed that shifts in allele frequencies in populations were the consequence of genetic drift rather than natural selection. This indicates that differences in the study populations, originating mainly from two seed zones (mixed wood and foothills; Supplementary Table S1), were not driven by adaptive evolution. We observed that the decoupling of functional tradeoffs varied in populations in the same test site, and found that this discrepancy was engendered by random evolutionary processes—genetic drift and gene flow. This indicates that random changes in allele frequency over time could affect resource allocation to phenotypic traits. In addition to evolutionary processes, plastic responses could drive phenotypic trait divergence of forest trees (Albert et al., 2011; Kawecki & Ebert, 2004). We found that all focal traits had strong plasticity across test sites, suggesting their ability to acclimate, but none of these traits showed significantly different plastic responses among families. This result could reflect either congruent selection on plasticity across families or constraints on the evolution of plasticity in focal traits in response to spatially heterogeneous selection.

Genetic basis of functional coordination

The use of a GBS method for genomic sequencing has the disadvantage of missing most variants across the genome (Lowry et al., 2017). Given conifer genome sizes of 20–30 Gb such as *P. taeda* of 22 Gb (https://treegenesdb.org/), the variant density of this study is equivalent to one SNP per 1 Mb. This sparse density of variants across the genome limits our ability to capture trait associative loci. Due to this limitation, we did not rely on identifying significantly associative variants but utilized a modeling approach based

on the signal strength of multi-trait peak associations to investigate genetic relationship of focal phenotypic traits. Moreover, we probed five SNPs with mean allele frequency difference of 0.55 between a cold (northernmost) and warm populations, indicating potential genetic tradeoffs, and found one SNP might relate to a dehydrogenase. In the future, we could experimentally test for genetic tradeoffs by demonstrating that alleles at the SNP or candidate gene have a fitness advantage in its home environment, but suffer a fitness cost when transplanted to a different environment (Mitchell-Olds et al., 2007).

In conclusion, by testing for the resource allocation hypothesis, identifying the cause of population divergence, and demonstrating genomic underpinnings of trait coordination based on four common-garden experiments for five lodgepole pine populations, the study integrated ecological, evolutionary, and genetic mechanisms to elucidate the ecological pattern, evolutionary drivers, and genetic basis of trait coordination, or rather, the decoupling of functional tradeoffs.

Supplementary material

Supplementary material is available online at *Evolution* (https://academic.oup.com/evolut/qpad004)

Data availability

The original genotyping data have been deposited on the SRA under the BioProject PRJNA715165. The raw phenotypic data and code have been archived on Borealis (Liu et al. 2022).

Author contributions

B.R.T., Y.A.E., and N.E. led and coordinated the project (experimental design and funding acquisition); X.W., J.G.K., A.U., B.R.T., and J.S.A. collected the phenotypic data; E.P.C., C.C., and B.R. pre-processed the phenotyping and genotyping data (variant calling); Y.L. conceived of this study, performed data analyses, wrote and revised the manuscript based on comments and direct inputs from N.E., Y.A.E., B.R.T., and the other co-authors. All authors read and approved the final manuscript.

Funding

This work was funded by Genome Canada, Genome Alberta through Alberta Economic Trade and Development, Genome British Columbia, the University of Alberta, the University of Calgary, the University of Cambridge, and the Australian Research Council Centre of Excellence for Plant Success in Nature and Agriculture (CE200100015).

Conflict of interest: The authors declare no conflict of interest.

Acknowledgments

We acknowledge funding provided by Alberta Innovates BioSolutions, Forest Resource Improvement Association of Alberta, the Forest Resource Improvement Program through West Fraser Ltd. (Blue Ridge Lumber and Hinton Wood Products) and Weyerhaeuser Timberlands (Grande Prairie and Pembina), Alberta Agriculture and Forestry, Blue Ridge Lumber West Fraser, Weyerhaeuser Timberlands Grande Prairie, and the Thomas, Wishart, and Erbilgin labs in support of the Resilient Forests (RES-FOR): Climate, Pests & Policy—Genomic Applications project. We are thankful to height trait contributors (B. R. Lumber and S. Sadoway), field/laboratory technicians (G. Ishangulyyeva, L. Vehring, and many summer students), and project manager (S. Bergheim) for providing altruistic support. In addition, we are grateful for the High-Performance Computing Center facilities at Oklahoma State University (NSF MRI-1531128), the Extreme Science and Engineering Discovery Environment (Bridges system; NSF ACI-1445606), and the UBC Advance Research Computing platform (ARC Sockeye) to afford extensive computational simulations. Finally, we appreciate suggestions and comments from two anonymous reviewers and the Editors, which have greatly strengthened the work.

References

Agrawal, A., Conner, J., & Rasmann, S. (2010). *Trade-offs and negative correlations in evolutionary ecology.* Sinauer Associates.

Aitken, S. N., & Bemmels, J. B. (2016). Time to get moving: Assisted gene flow of forest trees. *Evolutionary Applications*, 9, 271–290.

Albert, C. H., Grassein, F., Schurr, F. M., Vieilledent, G., & Violle, C. (2011). When and how should intraspecific variability be considered in trait-based plant ecology? *Perspectives in Plant Ecology Evolution and Systematics*, 13(3), 217–225. https://doi.org/10.1016/j.ppees.2011.04.003

Amman, G. D., & Baker, B. H. (1973). *Lodgepole pine losses to mountain pine beetle related to elevation* (General Technical Report INT-89). US Dept. of Agriculture, Forest Service, Intermountain Forest & Range Experiment Station. pp. 56.

Atkinson, N. J., & Urwin, P. E. (2012). The interaction of plant biotic and abiotic stresses: From genes to the field. *Journal of Experimental Botany*, 63(10), 3523–3543. https://doi.org/10.1093/jxb/ers100

Ballhorn, D. J. (2011). Constraints of simultaneous resistance to a fungal pathogen and an insect herbivore in lima bean (*Phaseolus lunatus* L.). *Journal of Chemical Ecology*, 37(2), 141–144. https://doi.org/10.1007/s10886-010-9905-0

Barton, K. E., & Koricheva, J. (2010). The ontogeny of plant defense and herbivory: Characterizing general patterns using meta-analysis. *American Naturalist*, 175, 481–493.

Bates, D., Machler, M., Bolker, B. M., & Walker, S. C. (2015). Fitting linear mixed effects models using lme4. *Journal of Statistical Software*, 67, 1–48.

Bentz, B. J., Régnière, J., Fettig, C. J., Hansen, E. M., Hayes, J. L., Hicke, J. A., Kelsey, R. G., Negrón J. F., & Seybold S. J. (2010). Climate change and bark beetles of the Western United States and Canada: Direct and indirect effects. *Bioscience*, 60(8), 602–613. https://doi.org/10.1525/bio.2010.60.8.6

Berner, L. T., Law, B. E., Meddens, A. J. H., & Hicke, J. A. (2017). Tree mortality from fires, bark beetles, and timber harvest during a hot and dry decade in the western United States (2003-2012). *Environmental Research Letters*, 12(6), 065005. https://doi.org/10.1088/1748-9326/aa6f94

Bigler, C., & Veblen, T. T. (2009). Increased early growth rates decrease longevities of conifers in subalpine forests. *Oikos*, 118(8), 1130–1138. https://doi.org/10.1111/j.1600-0706.2009.17592.x

Boege, K., Dirzo, R., Siemens, D., & Brown, P. (2007). Ontogenetic switches from plant resistance to tolerance: Minimizing costs with age?. *Ecology Letters*, 10, 177–187.

Bonello, P., Gordon, T. R., Herms, D. A., Wood, D. L., & Erbilgin, N. (2006). Nature and ecological implications of pathogen-induced systemic resistance in conifers: A novel hypothesis. *Physiological and Molecular Plant Pathology*, 68(4–6), 95–104. https://doi.org/10.1016/j.pmpp.2006.12.002

Boone, C. K., Aukema, B. H., Bohlmann, J., Carroll, A. L., & Raffa, K. F. (2011). Efficacy of tree defense physiology varies with bark beetle population density: A basis for positive feedback in eruptive species. *Canadian Journal of Forest Research*, 41, 1174–1188.

Caicedo, A. L., Stinchcombe, J. R., Olsen, K. M., Schmitt, J., & Purugganan, M. D. (2004). Epistatic interaction between *Arabidopsis FRI* and *FLC* flowering time genes generates a latitudinal cline in a life history trait. *Proceedings of the National Academy of Sciences of the USA*, 101(44), 15670–15675. https://doi.org/10.1073/pnas.0406232101

Capblancq, T., Luu, K., Blum, M. G. B., & Bazin, E. (2018). Evaluation of redundancy analysis to identify signatures of local adaptation. *Molecular Ecology Resources*, 18(6), 1223–1233. https://doi.org/10.1111/1755-0998.12906

Chapman, J. W., Reynolds, D. R., & Wilson, K. (2015). Long-range seasonal migration in insects: Mechanisms, evolutionary drivers and ecological consequences. *Ecology Letters*, 18(3), 287–302. https://doi.org/10.1111/ele.12407

Chen, C., Mitchell, S. E., Elshire, R. J., Buckler, E. S., & El-Kassaby, Y. A. (2013). Mining conifers' mega-genome using rapid and efficient multiplexed high-throughput genotyping-by-sequencing (GBS) SNP discovery platform. *Tree Genetics & Genomes*, 9, 1537–1544.

Coley, P. D., Bryant, J. P., & Chapin, F. S., 3rd (1985). Resource availability and plant antiherbivore defense. *Science*, 230, 895–899.

Colhoun, J. (1973). Effects of environmental factors on plant disease. *Annual Review of Phytopathology*, 11(1), 343–364. https://doi.org/10.1146/annurev.py.11.090173.002015

Cumbie, W. P., Eckert, A., Wegrzyn, J., Whetten, R., Neale, D., & Goldfarb, B. (2011). Association genetics of carbon isotope discrimination, height and foliar nitrogen in a natural population of *Pinus taeda* L. *Heredity*, 107(2), 105–114. https://doi.org/10.1038/hdy.2010.168

Damgaard, C. (2019). A critique of the space-for-time substitution practice in community ecology. *Trends in Ecology and Evolution*, 34(5), 416–421. https://doi.org/10.1016/j.tree.2019.01.013

Dray, S., & Dufour, A.-B. (2007). The ade4 package: Implementing the duality diagram for ecologists. *Journal of Statistical Software*, 22, 1–20.

Elshire, R. J., Glaubitz, J. C., Sun, Q., Poland, J. A., Kawamoto, K., Buckler, E. S., & Mitchell, S. E. (2011). A robust, simple genotyping-by-sequencing (GBS) approach for high diversity species. *PLoS One*, 6(5), e19379. https://doi.org/10.1371/journal.pone.0019379

Endara, M. J., & Coley, P. D. (2011). The resource availability hypothesis revisited: A meta-analysis. *Functional Ecology*, 25, 389–398.

Erb, M., Balmer, D., De Lange, E. S., Von Merey, G., Planchamp, C., Robert, C. A., Röder, G., Sobhy, I., Zwahlen, C., Mauch-Mani, B., & Turlings, T. C. 2011. Synergies and trade-offs between insect and pathogen resistance in maize leaves and roots. *Plant, Cell & Environment*, 34,1088–1103.

Erb, M., Meldau, S., & Howe, G. A. (2012). Role of phytohormones in insect-specific plant reactions. *Trends in Plant Science*, 17(5), 250–259. https://doi.org/10.1016/j.tplants.2012.01.003

Erbilgin, N. (2019). Phytochemicals as mediators for host range expansion of a native invasive forest insect herbivore. *New Phytologist*, 221, 1268–1278.

Erbilgin, N., Zanganeh, L., Klutsch, J. G., Chen, S. H., Zhao, S., Ishangulyyeva, G., Burr, S. J., Gaylord, M., Hofstetter, R., Keefover-Ring, K., Raffa, K. F., & Kolb. T. (2021). Combined drought and bark beetle attacks deplete non-structural carbohydrates and promote death of mature pine trees. *Plant, Cell & Environment*, 44, 3636–3651.

Fardusi, M. J., Ferrio, J. P., Comas, C., Voltas, J., Resco de Dios, V., & Serrano, L. (2016). Intra-specific association between carbon isotope composition and productivity in woody plants: A meta-analysis. *Plant Science*, 251, 110–118. https://doi.org/10.1016/j.plantsci.2016.04.005

Fine, P. V. A., Mesones, I., & Coley, P. D. (2004). Herbivores promote habitat specialization by trees in Amazonian forests. *Science*, 305(5684), 663–665. https://doi.org/10.1126/science.1098982

Forester, B. R., Lasky, J. R., Wagner, H. H., & Urban, D. L. (2018). Comparing methods for detecting multilocus adaptation with multivariate genotype-environment associations. *Molecular Ecology*, 27(9), 2215–2233. https://doi.org/10.1111/mec.14584

Franceschi, V. R., Krokene, P., Christiansen, E., & Krekling, T. (2005). Anatomical and chemical defenses of conifer bark against bark beetles and other pests. *New Phytologist*, 167(2), 353–376. https://doi.org/10.1111/j.1469-8137.2005.01436.x

Galmán, A., Abdala-Roberts, L., Zhang, S., Berny-Mier y Teran, J. C., Rasmann, S., & Moreira, X. (2018). A global analysis of elevational gradients in leaf herbivory and its underlying drivers: Effects of plant growth form, leaf habit and climatic correlates. *Journal of Ecology*, 106, 413–421.

Gavrilets, S., & Scheiner, S. M. (1993). The genetics of phenotypic plasticity. V. Evolution of reaction norm shape. *Journal of Evolutionary Biology*, 6(1), 31–48. https://doi.org/10.1046/j.1420-9101.1993.6010031.x

Glaubitz, J. C., Casstevens, T. M., Lu, F., Harriman, J., Elshire, R. J., Sun, Q., & Buckler, E. S. (2014). TASSEL-GBS: A high capacity genotyping by sequencing analysis pipeline. *PLoS One*, 9(2), e90346. https://doi.org/10.1371/journal.pone.0090346

Gornall, J. L., & Guy, R. D. (2007). Geographic variation in ecophysiological traits of black cottonwood (*Populus trichocarpa*). *Canadian Journal of Botany*, 85(12), 1202–1213. https://doi.org/10.1139/b07-079

Grime, J. P. (1979). *Plant strategies and vegetation processes*. John Wiley and Sons.

Hicke, J. A., Allen, C. D., Desai, A. R., Dietze, M. C., Hall, R. J., Hogg, E. H.,… Vogelmann, J. (2012). Effects of biotic disturbances on forest carbon cycling in the United States and Canada. *Global Change Biology,* 18, 7–34.

Huang, J. B., Kautz, M., Trowbridge, A. M., Hammerbacher, A., Raffa, K. F., Adams, H. D., Goodsman, D. W., Xu, C. G., Meddens, A. J. H., Kandasamy, D., Gershenzon, J., Seidl, R., & Hartmann, H. (2020). Tree defence and bark beetles in a drying world: Carbon partitioning, functioning and modelling. *New Phytologist*, 225, 26–36.

Hussain, A., Classens, G., Guevara-Rozo, S., Cale, J. A., Rajabzadeh, R., Peters, B. R., & Erbilgin, N. (2020). Spatial variation in soil available water holding capacity alters carbon mobilization and allocation to chemical defenses along jack pine stems. *Environmental and Experimental Botany*, 171, 103902. https://doi.org/10.1016/j.envexpbot.2019.103902

Jamieson, M. A., Trowbridge, A. M., Raffa, K. F., & Lindroth, R. L. (2012). Consequences of climate warming and altered precipitation patterns for plant-insect and multitrophic interactions. *Plant Physiology*, 160(4), 1719–1727. https://doi.org/10.1104/pp.112.206524

Karasov, T. L., Chae, E., Herman, J. J., & Bergelson, J. (2017). Mechanisms to mitigate the trade-off between growth and defense. *Plant Cell*, 29(4), 666–680. https://doi.org/10.1105/tpc.16.00931

Karhunen, M., & Ovaskainen, O. (2012). Estimating population-level coancestry coefficients by an admixture F model. *Genetics*, 192(2), 609–617. https://doi.org/10.1534/genetics.112.140871

Kawecki, T. J., & Ebert, D. (2004). Conceptual issues in local adaptation. *Ecology Letters*, 7, 1225–1241.

Kelly, C. A. (1992). Spatial and temporal variation in selection on correlated life-history traits and plant size in *Chamaecrista fasciculata*. *Evolution*, 46(6), 1658–1673. https://doi.org/10.2307/2410022

Kempel, A., Schädler, M., Chrobock, T., Fischer, M., & Kleunen, M. van (2011). Tradeoffs associated with constitutive and induced plant resistance against herbivory. *Proceedings of the National Academy of Sciences of the USA*, 108, 5685–5689.

Kichas, N. E., Trowbridge, A. M., Raffa, K. F., Malone, S. C., Hood, S. M., Everett, R. G., McWethy, D. B., & Pederson, G. T. (2021). Growth and defense characteristics of whitebark pine (*Pinus albicaulis*) and lodgepole pine (*Pinus contorta var latifolia*) in a high-elevation, disturbance-prone mixed-conifer forest in northwestern Montana, USA. *Forest Ecology and Management,* 493, 119286.

Kolb, T. E., Fettig, C. J., Ayres, M. P., Bentz, B. J., Hicke, J. A., Mathiasen, R., Stewart, J. E., & Weed, A. S. (2016). Observed and anticipated impacts of drought on forest insects and diseases in the United States. *Forest Ecology and Management*, 380, 321–334.

Kolb, T., Keefover-Ring, K., Burr, S. J., Hofstetter, R., Gaylord, M., & Raffa, K. F. (2019). Drought-mediated changes in tree physiological processes weaken tree defenses to bark beetle attack. *Journal of Chemical Ecology*, 45(10), 888–900. https://doi.org/10.1007/s10886-019-01105-0

Kolosova, N., & Bohlmann, J. (2012). Conifer defense against insects and fungal pathogens. In R. Matyssek, H. Schnyder, W. Oßwald, D. Ernst, J. Munch, & H. Pretzsch (Eds.), *Growth and defence in plants: Resource allocation at multiple scales* (pp. 85–108). Springer-Verlag.

Kuznetsova, A., Brockhoff, P. B., & Christensen, R. H. B. (2017). lmerTest Package: Tests in linear mixed effects models. *Journal of Statistical Software*, 82, 1–26.

Lande, R. (1979). Quantitative genetic analysis of multivariate evolution, applied to brain: Body size allometry. *Evolution*, 33(1), 402–416. https://doi.org/10.2307/2407630

Lande, R. (1980). The genetic covariance between characters maintained by pleiotropic mutations. *Genetics*, 94(1), 203–215. https://doi.org/10.1093/genetics/94.1.203

Lê, S., Josse, J., & Husson, F. (2008). FactoMineR: An R package for multivariate analysis. *Journal of Statistical Software*, 25, 1–18.

Legendre, L., & Legendre, L. (1998). *Numerical ecology*. Elsevier.

Leites, L. P., Rehfeldt, G. E., & Steiner, K. C. (2019). Adaptation to climate in five eastern North America broadleaf deciduous species: Growth clines and evidence of the growth-cold tolerance tradeoff. *Perspectives in Plant Ecology Evolution and Systematics*, 37, 64–72. https://doi.org/10.1016/j.ppees.2019.02.002

Li, H., & Durbin, R. (2009). Fast and accurate short read alignment with Burrows-Wheeler transform. *Bioinformatics*, 25(14), 1754–1760. https://doi.org/10.1093/bioinformatics/btp324

Liu, Y., Erbilgin, N., Cappa, E. P., Chen, C., Ratcliffe, B., Wei, X., Klutsch, J. G., Ullah, A., Azcona, J. S., Thomas, B. R., & El-Kassaby, Y. A. (2022). "Data from: Decoupling of height growth and drought or pest resistance tradeoffs is revealed through multiple common-garden experiments of lodgepole pine." *UBC Research Data Collection*. DOI: https://doi.org/10.5683/SP3/3UAXS9.

Lind, E. M., Borer, E., Seabloom, E., Adler, P., Bakker, J. D., Blumenthal, D. M., Crawley, M., Davies, K., Firn, J., Gruner, D. S., Stanley, H. W., Hautier, Y., Hillebrand, H., Knops, J., Melbourne, B., Mortensen, B., Risch, A. C., Schuetz, M., Stevens, C.,…Wragg, P. D. (2013). Life-history constraints in grassland plant species: A growth-defence trade-off is the norm. *Ecology Letters*, 16(4), 513–521. https://doi.org/10.1111/ele.12078

Liu, X., Huang, M., Fan, B., Buckler, E. S., & Zhang, Z. (2016). Iterative usage of fixed and random effect models for powerful and efficient genome-wide association studies. *PLoS Genetics*, 12(2), e1005767. https://doi.org/10.1371/journal.pgen.1005767

Lowry, D. B., Hoban, S., Kelley, J. L., Lotterhos, K. E., Reed, L. K., Antolin, M. F., & Storfer, A. (2017). Breaking RAD: An evaluation of the utility of restriction site-associated DNA sequencing for genome scans of adaptation. *Molecular Ecology Resources*, 17, 142–152.

Mason, C. J., Keefover-Ring, K., Villari, C., Klutsch, J. G., Cook, S., Bonello, P., Erbilgin, N., Raffa, K. F., & Townsend, P. A. 2019. Anatomical defences against bark beetles relate to degree of historical exposure between species and are allocated independently of chemical defences within trees. *Plant, Cell & Environment*, 42, 633–646.

McDowell, N. G., Beerling, D. J., Breshears, D. D., Fisher, R. A., Raffa, K. F., & Stitt, M. (2011). The interdependence of mechanisms underlying climate-driven vegetation mortality. *Trends in Ecology and Evolution*, 26(10), 523–532. https://doi.org/10.1016/j.tree.2011.06.003

McKown, A. D., Guy, R. D., Quamme, L., Klápště, J., La Mantia, J., Constabel, C. P., El-Kassaby, Y. A., Hamelin, R. C., Zifkin, M., & Azam, M. S. (2014). Association genetics, geography and ecophysiology link stomatal patterning in *Populus trichocarpa* with carbon gain and disease resistance trade-offs. *Molecular Ecology*, 23(23), 5771–5790. https://doi.org/10.1111/mec.12969

Mitchell-Olds, T., Willis, J. H., & Goldstein, D. B. (2007). Which evolutionary processes influence natural genetic variation for phenotypic traits?. *Nature Reviews Genetics*, 8, 845–856.

Moran, N. A. (1992). The evolutionary maintenance of alternative phenotypes. *American Naturalist*, 139(5), 971–989. https://doi.org/10.1086/285369

Mullin, M., Klutsch, J. G., Cale, J. A., Hussain, A., Zhao, S., Whitehouse, C., & Erbilgin, N. (2021). Primary and secondary metabolite profiles of lodgepole pine trees change with elevation, but not with latitude. *Journal of Chemical Ecology*, 47(3), 280–293. https://doi.org/10.1007/s10886-021-01249-y

Nakagawa, S., & Schielzeth, H. (2013). A general and simple method for obtaining R^2 from generalized linear mixed-effects models. *Methods in Ecology and Evolution*, 4, 133–142.

Niinemets, U. (2010). A review of light interception in plant stands from leaf to canopy in different plant functional types and in species with varying shade tolerance. *Ecological Research*, 25(4), 693–714. https://doi.org/10.1007/s11284-010-0712-4

Nychka, D., Bandyopadhyay, S., Hammerling, D., Lindgren, F., & Sain, S. (2015). A multiresolution Gaussian process model for the analysis of large spatial datasets. *Journal of Computational and Graphical Statistics*, 24, 579–599.

Oksanen, J., Blanchet, F. G., Friendly, M., Kindt, R., Legendre, P., McGlinn, D., Minchin, P. R., O'Hara, R. B., Simpson, G. L., Solymos, P., Stevens, M. H. H., Szoecs, E., & Wagner, H. 2017. *vegan: Community ecology package. R package version 2.5-6*. Avaiable at https://CRAN.R-project.org/package=vegan

Ovaskainen, O., Karhunen, M., Zheng, C. Z., Arias, J. M. C., & Merilä, J. (2011). A new method to uncover signatures of divergent and stabilizing selection in quantitative traits. *Genetics*, 189, 621–632.

Pickett, S. T. A. (1989). Space-for-time substitution as an alternative to long-term studies. In G. E. Likens (Ed.), *Long-term studies in ecology: Approaches and alternatives* (pp. 110–135). Springer New York.

Price, A. L., Patterson, N. J., Plenge, R. M., Weinblatt, M. E., Shadick, N. A., & Reich, D. (2006). Principal components analysis corrects for stratification in genome-wide association studies. *Nature Genetics*, 38(8), 904–909. https://doi.org/10.1038/ng1847

R Core Team. (2020). *R: A language and environment for statistical computing*. R Foundation for Statistical Computing.

Raffa, K. F., Aukema, B. H., Bentz, B. J., Carroll, A. L., Hicke, J. A., Turner, M. G., & Romme, W. H. (2008). Cross-scale drivers of natural disturbances prone to anthropogenic amplification: The dynamics of bark beetle eruptions. *Bioscience*, 58(6), 501–517. https://doi.org/10.1641/b580607

Raffa, K. F., Aukema, B. H., Erbilgin, N., Klepzig, K. D., & Wallin, K. F. (2005). Interactions among conifer terpenoids and bark beetles across multiple levels of scale: An attempt to understand links between population patterns and physiological processes. *Recent Advances in Phytochemistry*, 39, 79–118.

Raffa, K. F., Mason, C. J., Bonello, P., Cook, S., Erbilgin, N., Keefover-Ring, K., Klutsch, J. G., Villari, C., & Townsend, P. A. (2017). Defence syndromes in lodgepole – whitebark pine ecosystems relate to degree of historical exposure to mountain pine beetles. *Plant, Cell & Environment*, 40(9), 1791–1806. https://doi.org/10.1111/pce.12985

Ramírez-Valiente, J. A., López, R., Hipp, A. L., & Aranda, I. (2020). Correlated evolution of morphology, gas exchange, growth rates and hydraulics as a response to precipitation and temperature regimes in oaks (*Quercus*). *New Phytologist*, 227, 794–809.

Rose, M. R. (1983). Further models of selection with antagonistic pleiotropy. In H. I. Freedman, & C. Strobeck, (Eds.), *Population biology* (pp. 47–53). Springer.

Sala, A., Woodruff, D. R., & Meinzer, F. C. (2012). Carbon dynamics in trees: Feast or famine?. *Tree Physiology*, 32(6), 764–775. https://doi.org/10.1093/treephys/tpr143

Schielzeth, H., & Nakagawa, S. (2013). Nested by design: Model fitting and interpretation in a mixed model era. *Methods in Ecology and Evolution*, 4, 14–24.

Schluter, D., Price, T. D., & Rowe, L. (1991). Conflicting selection pressures and life-history trade-offs. *Proceedings of the Royal Society B: Biological Sciences*, 246, 11–17.

Solovieff, N., Cotsapas, C., Lee, P. H., Purcell, S. M., & Smoller, J. W. (2013). Pleiotropy in complex traits: Challenges and strategies. *Nature Reviews Genetics*, 14(7), 483–495. https://doi.org/10.1038/nrg3461

Stearns, S. C. (1999). *The evolution of life histories*. Oxford University Press.

Stinchcombe, J. R., Weinig, C., Ungerer, M., Olsen, K. M., Mays, C., Halldorsdottir, S. S., Purugganan, M. D., & Schmitt, J. (2004). A latitudinal cline in flowering time in *Arabidopsis thaliana* modulated by the flowering time gene *FRIGIDA*. *Proceedings of the National Academy of Sciences of the United States of America*, 101(13), 4712–4717. https://doi.org/10.1073/pnas.0306401101

Stoffel, M. A., Nakagawa, S., & Schielzeth, H. (2017). rptR: Repeatability estimation and variance decomposition by generalized linear mixed-effects models. *Methods in Ecology and Evolution*, 8(11), 1639–1644. https://doi.org/10.1111/2041-210x.12797

Strauss, S. Y., Rudgers, J. A., Lau, J. A., & Irwin, R. E. (2002). Direct and ecological costs of resistance to herbivory. *Trends in Ecology and Evolution*, 17(6), 278–285. https://doi.org/10.1016/s0169-5347(02)02483-7

Tenkanen, A., Keski-Saari, S., Salojärvi, J., Oksanen, E., Keinänen, M., & Kontunen-Soppela, S. (2019). Differences in growth and gas exchange between southern and northern provenances of silver birch (*Betula pendula* Roth) in northern Europe. *Tree Physiology*, 40(2), 198–214. https://doi.org/10.1093/treephys/tpz124

Trumbore, S., Brando, P., & Hartmann, H. (2015). Forest health and global change. *Science*, 349(6250), 814–818. https://doi.org/10.1126/science.aac6759

Ullah, A., Klutsch, J. G., & Erbilgin, N. (2021). Production of complementary defense metabolites reflects a co-evolutionary arms race between a host plant and a mutualistic bark beetle-fungal complex. *Plant Cell and Environment*, 44(9), 3064–3077. https://doi.org/10.1111/pce.14100

VanRaden, P. M. (2008). Efficient methods to compute genomic predictions. *Journal of Dairy Science*, 91, 4414–4423.

Venables, W. N., & Ripley, B. D. (2002). *Modern applied statistics with S*. Springer.

Wang, T. L., Hamann, A., Spittlehouse, D., & Carroll, C. (2016). Locally downscaled and spatially customizable climate data for historical and future periods for North America. *PLoS One*, 11, e0156720.

Wood, S. N. (2011). Fast stable restricted maximum likelihood and marginal likelihood estimation of semiparametric generalized linear models. *Journal of the Royal Statistical Society. Series B (Statistical Methodology)*, 73, 3–36.

Wright, S. J., Muller-Landau, H. C., Condit, R., & Hubbell, S. P. (2003). Gap-dependent recruitment, realized vital rates, and size distributions of tropical trees. *Ecology*, 84(12), 3174–3185. https://doi.org/10.1890/02-0038

Xu, Z. H., Saffigna, P. G., Farquhar, G. D., Simpson, J. A., Haines, R. J., Walker, S., Osborne, D. O., & Guinto, D. (2000). Carbon isotope discrimination and oxygen isotope composition in clones of the F_1 hybrid between slash pine and Caribbean pine in relation to tree growth, water-use efficiency and foliar nutrient concentration. *Tree Physiology*, 20(18), 1209–1217. https://doi.org/10.1093/treephys/20.18.1209

Zangerl, A. R., & Rutledge, C. E. (1996). The probability of attack and patterns of constitutive and induced defense: A test of optimal defense theory. *American Naturalist*, 147(4), 599–608. https://doi.org/10.1086/285868

Züst, T., & Agrawal, A. A. (2017). Trade-offs between plant growth and defense against insect herbivory: An emerging mechanistic synthesis. *Annual Review of Plant Biology*, 68(1), 513–534. https://doi.org/10.1146/annurev-arplant-042916-040856

Züst, T., Heichinger, C., Grossniklaus, U., Harrington, R., Kliebenstein, D. J., & Turnbull, L. A. (2012). Natural enemies drive geographic variation in plant defenses. *Science*, 338(6103), 116–119. https://doi.org/10.1126/science.1226397